Dyes and Pigments 95 (2012) 534–539

Contents lists available at SciVerse ScienceDirect

Dyes and Pigments

journal homepage: www.elsevier.com/locate/dyepig

Low temperature synthesis and characterization of rutile TiO_2-coated mica–titania pigments

Qiang Gao [a,b], Xiaomei Wu [a,b,*], Yueming Fan [a,b], Xiya Zhou [a,b]

[a] School of Materials Science and Engineering, South China University of Technology, Guangzhou 510641, People's Republic of China
[b] Key Laboratory of Specially Functional Materials of the Ministry of Education, South China University of Technology, Guangzhou 510641, People's Republic of China

ARTICLE INFO

Article history:
Received 7 April 2012
Received in revised form
9 June 2012
Accepted 13 June 2012
Available online 21 June 2012

Keywords:
Pearlescent pigment
Anatase–rutile transformation
MnO_2
TiO_2
Photocatalytic
Mica

ABSTRACT

Rutile TiO_2-coated mica–titania pigments were prepared by hydrolysis of $TiCl_4$ ethanolic solution in water at 70 °C. MnO_2 as a rutile promoting additive was deposited onto mica prior to TiO_2. X-ray diffraction and Raman spectra analysis verified that use of only 2.07 wt% MnO_2 with respect to mica weight began to provide a complete rutile TiO_2 coating without calcination. The rutile promoting effects of MnO_2 could be ascribed to the structural similarity of rutile and pyrolusite. Scanning electron microscopy analysis showed that MnO_2 also had a pronounced effect on the morphology of TiO_2 coatings. The prior deposition of MnO_2 onto mica lead to the formation of rutile TiO_2 films composed of highly oriented fine needles on the mica surface and nanoflower structures on the needle structures. The as-obtained rutile-TiO_2 coated mica–titanium pigments are shown to exhibit a high photostability under UV illumination.

1. Introduction

Pearlescent pigments, which can be natural or synthetic, show outstanding qualities of luster, brilliance and iridescent color effects resulting from light interference or multiple reflections [1,2]. These pigments are synthesized by coating low refractive index materials like mica and silica, with high refractive index materials such as metal oxides [3]. The metal oxides often used for coating are TiO_2, Fe_2O_3, Cr_2O_3, SnO_2, ZnO, ZrO_2 or a complex of these oxides [4,5].

Pearlescent pigments are widely applied for functional and decorative purposes, such as optical filters, cosmetics, plastics, printed products, ceramic, industrial coatings, and car paints for their effects [6–10]. Some have also been used due to such properties as electrical conductivity, magnetic properties and IR reflection [11–13]. The best known examples are mica–titania pigments that are based on TiO_2 precipitated onto platelets of mica [5].

There are various methods for depositing TiO_2 onto mica flakes, including homogeneous hydrolysis, titration, sol–gel technique, and chemical vapor deposition [1,11,14,15]. Calcinations at 800 °C to 900 °C convert the amorphous TiO_2 precipitate to crystalline TiO_2 thin layer [2]. It is well known that TiO_2 is a polymorphous compound, crystallizing as: rutile, anatase, or brookite. All of these polymorphs have the same fundamental structural octahedral units with different arrangements [16]. In contrast with the other two phases, rutile TiO_2 is the most stable phase even in strongly acidic or basic conditions [17]. The refractive index of rutile (2.93) is higher than that of anatase (2.488), so that the effect of strong color and luster can be achieved when mica–titania pigments consist of complete rutile layers [18]. Furthermore, rutile has been found to show poor photocatalytic activities in most case [19,20], which may help to solve the problem of 'chalking' (photooxidation of surrounding polymeric binders in outdoor weathering initiated by the pigment) that has been besetting the coatings industry [21–23]. For the foregoing reasons, rutile modification of titanium dioxide in a pearlescent pigment is more desirable than the anatase modification.

The synthesis of phase-pure rutile form under low temperature is generally believed to be very difficult because most of the techniques adopted for the synthesis of titania produce the kinetically favorable polymorph of anatase [16,24]. Moreover, due to the anatase directing effect of mica [25], anatase still exist

* Corresponding author. School of Materials Science and Engineering, South China University of Technology, Guangzhou 510641, People's Republic of China. Tel./fax: +86 020 87114243.
E-mail addresses: imxmeiwu@scut.edu.cn, johnsongao2010@hotmail.com (X. Wu).

0143-7208/$ – see front matter © 2012 Elsevier Ltd. All rights reserved.
http://dx.doi.org/10.1016/j.dyepig.2012.06.006

Table 1
Elemental analysis of materials.

Sample	Component (wt %)									
	TiO_2	SiO_2	MgO	Al_2O_3	K_2O	F	Na_2O	MnO_2	Fe_2O_3	CeO_2
mica–TiO_2	32.61	29.45	19.71	8.8	6.49	2.21	0.4	–	0.05	0.13
mica-2.07%MnO_2–TiO_2	47.92	22.51	15.41	6.92	5.18	1.35	–	0.31	0.07	0.13

when the calcination temperature increases to 1000 °C [18,26]. Rutile modification of mica–titania pigments can be obtained via doping and high-temperature calcination as we reported previously [27]. However, high-temperature calcination leads to the formation of cracks in the coating layer, finally leading to the decline of pearl luster [5,26,28]. So fabrication of rutile TiO_2 coated mica–titania pigments at low temperatures is a great challenge.

In this paper, a novel method of depositing rutile TiO_2 onto a mica substrate at 70 °C without calcinations was described. Rutile TiO_2 coated mica–titania pigments were synthesized by hydrolysis of titanium tetrachloride and the effect of MnO_2 on the anatase–rutile transformation was investigated.

2. Experimental

2.1. Materials

The mica used as the substrate in this study was synthetic mica, supplied by Sanbao Pearl Luster Mica Tech CO., LTD, China. Dry mica flakes were sieved to obtain narrow size distribution. Analytical grade titanium tetrachloride ($TiCl_4$), manganese chloride ($MnCl_2$), absolute ethanol (C_2H_5OH), sodium hydroxide (NaOH), and hydrochloric acid (HCl) were used in the experiments, throughout which distilled water was used.

The starting material in this study to deposit TiO_2 layer on mica was $TiCl_4$ ethanolic solution. In general, concentrated $TiCl_4$ gives a sudden reaction with water at room temperature, and $Ti(OH)_4$ forms [29]. In order to prevent such formation, $TiCl_4$ was added dropwise into absolute ethanol to obtain the precursor. The main components of the precursor are $TiCl_x(OCH_2CH_3)_{4-x}$ complex species [30].

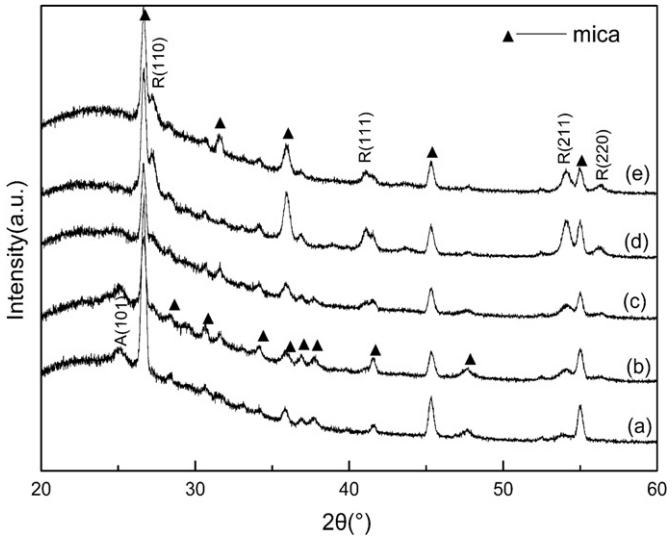

Fig. 1. XRD patterns of mica–titania pigments with different amounts of MnO_2: (a) mica–TiO_2, (b) mica-0.69% MnO_2–TiO_2, (c) mica-1.38% MnO_2–TiO_2, (d) mica-2.07% MnO_2–TiO_2, (e) mica-2.76% MnO_2–TiO_2.

2.2. Preparation method

2.2.1. Preparation of pure mica–titania pigments

The preparation of pure mica–titania pigments was carried out in the following way [18,31]. First, 10 g of mica was dispersed with 1 L distilled water. The batch was then heated to 70 °C under stirring and pH value was adjusted to 1.0 with diluted hydrochloric acid. Then 0.120 L precursor was introduced into the agitated slurry at a constant speed of 0.5 mL/min. The pH value of the slurry was kept constant by simultaneous addition of NaOH solution. After the addition was completed, the slurry was aged for 1 h and then allowed to settle and cool to room temperature. Lastly, the particles were separated, washed with distilled water, and dried at 70 °C for 24 h. This sample was labeled as mica–TiO_2.

2.2.2. Preparation of mica–titania pigments with a prior deposition of MnO_2

The introduction of MnO_2 in order to obtain rutile phase of TiO_2 onto mica substrate was achieved using $MnCl_2$ solution. First, mica was suspended in distilled water and heated to 70 °C, and the pH value of the slurry was adjusted to 2.0 using HCl. Then, $MnCl_2$ aqueous solution (15 g/L) was added dropwise while the pH value was held constant by simultaneous addition of NaOH solution for 1 h. Weight ratios of MnO_2 to mica were 0.69%, 1.38%, 2.07% and 2.76% respectively. Then, the pH value was adjusted to 1.0, and the TiO_2 coating was deposited on mica by addition of precursor the same way as described in 2.2.1. The final samples were labeled as mica-x% MnO_2–TiO_2 (x = 0.69, 1.38, 2.07 or 2.76).

2.3. Characterization

2.3.1. X-ray diffraction analysis

X-ray powder diffraction (XRD) analysis was performed using a PANalytical X'Pert Pro diffractometer using Cu Kα radiation at

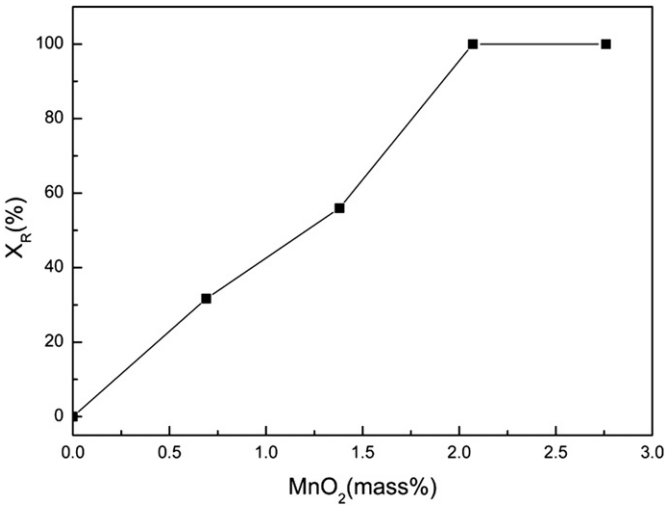

Fig. 2. Mass fraction of rutile phase of the mica–titania pigments with different MnO_2 loadings.

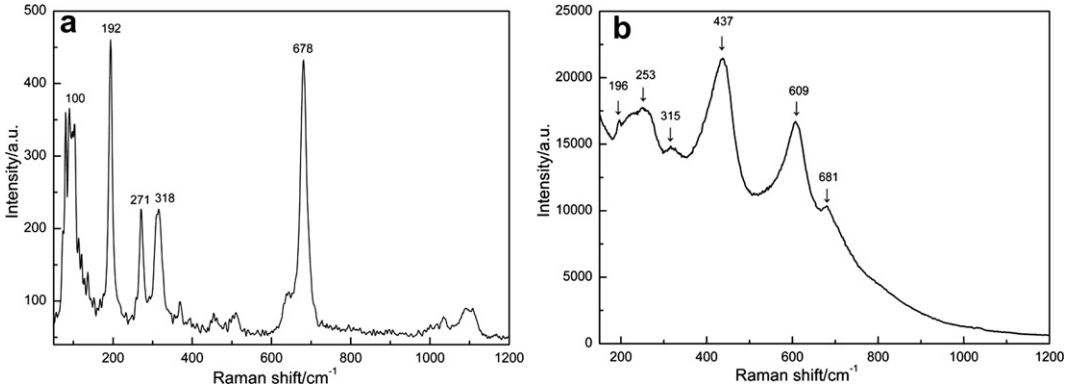

Fig. 3. Raman spectra of (a) mica and (b) mica-2.07%MnO_2–TiO_2.

40 kV and 40 mA for the crystal structure determination of TiO_2 on mica. XRD patterns were recorded in the 2θ range from 20° to 60° with a step size of 0.01° and a scan step time of 0.3 s.

The percentages of anatase and rutile in the TiO_2 layer were calculated from X-ray powder diffraction intensities corresponding to anatase (101) and rutile (110) reflections. Then, the mass fraction of rutile, X_R, was determined by following equation [32,33].

$$X_R = \frac{1}{1 + 1.26(I_A/I_R)} \times 100\% \quad (1)$$

where I_A and I_R are the intensities of anatase (101) reflection and rutile (110) refection, respectively.

2.3.2. Scanning electron microscopy analysis

The samples were examined by scanning electron microscopy (SEM, Nova NanoSEM 430, FEI Company) to characterize the morphology of TiO_2 coatings. The operation voltage was 10 kV.

2.3.3. X-ray fluorescence spectrometry analysis

Chemical composition of mica–titanium pigments was determined by X-ray fluorescence spectrometry using a model PANalytical Axios.

2.3.4. Raman spectroscopy analysis

Raman spectroscopy was done on a LabRAM Aramis (HORIBA Jobin Yvon) with spectral resolution of 1 cm^{-1}. The laser line of the exciting source was at 532 nm.

2.3.5. Optical properties

To investigate the optical properties of the pigments, the pigment powders were pressed into a wafer with a diameter of 1.5 mm. Then, the spectral reflectance and the CIE $L^*a^*b^*$ of the pigment samples under 10°were measured by the X-Rite Inc model spectrophotometer (D65 illuminant).

2.3.6. Photocatalytic activity test

The photocatalytic activities of the samples were evaluated by the degradation of Rhodamine B (RhB) in an aqueous solution. Each sample containing 150 mg of TiO_2 was suspended in a 150 mL of aqueous solution of 20 mg/L RhB. The solution was continuously stirred for about 1 h to ensure the establishment of an absorption–desorption equilibrium among the pigments, RhB, and water before irradiation. Then the solution was illuminated by a 160 W high pressure mercury lamp (Philips, UV wave-length of the maximum intensity: 365 nm) in a black box. The distance between light source and the top of the solution was about 10 cm. The concentration of RhB solution was monitored by using a Cary 60 UV–VIS spectrophotometer (Agilent Ltd.)

3. Results and discussion

3.1. The effect of MnO_2 on the anatase–rutile (A–R) transformation

Table 1 presents the chemical composition of mica–TiO_2 and mica-2.07%MnO_2–TiO_2 determined by XRF. SiO_2, Al_2O_3 and MgO are the main components of mica. The loading of TiO_2 in mica–MnO_2–TiO_2 is higher than that of mica–TiO_2. The reason may be that the prior deposition of MnO_2 increases the surface roughness of mica, and higher surface roughness favors the absorption of TiO_2 nuclei onto mica surface.

The XRD patterns of mica–titania pigments prepared with different amounts of MnO_2 are shown in Fig. 1. The XRD peaks appearing at $2\theta = 25.1°$ corresponds to (001) plane of anatase TiO_2 (JCPDS 21-1272) and the XRD peaks with 2θ values of 27.1, 40.9°, 54.0°, 56.2° correspond to (110), (111), (211), (220) planes of rutile TiO_2 (JCPDS 21-1276). It is found that when the sample is not treated with any additives, only anatase appears (Fig. 1(a)). However, the peaks of rutile phase appear when mica particles are deposited with MnO_2. Then the intensity of rutile increases and the peaks of rutile sharpen with increasing loadings of MnO_2 while the intensity of anatase decreases. When the loading of MnO_2 is increased to 2.07%, the TiO_2 in the mica–titania pigments is in the rutile phase, so anatase transforms to rutile completely.

Fig. 2 shows the graphical illustration of the change of mass fraction of rutile phase with varying MnO_2 loadings. It is clear that the mass fraction of rutile phase goes up gradually with increasing MnO_2 loadings, which is followed by a leveling off at 100%.

In order to further confirm the surface coating is in rutile phase, Raman spectroscopy was used. The anatase and rutile phase of TiO_2 can be sensitively identified by Raman spectroscopy based on their Raman spectra. The major Raman bands of anatase phase are at 144, 197, 399, 515, and 639 cm^{-1}. These bands can be attributed to the five Raman-active modes of anatase phase with the symmetries of E_g, E_g (low-frequency), B_{1g}, A_{1g}, and E_g (high-frequency), respectively [34,35]. The typical Raman bands of rutile phase appear at 143, 235, 447, 612 cm^{-1}, which can be ascribed to the B_{1g}, two-photo scattering, E_g, and A_{1g} modes, respectively [36,37]. As can

Table 2
The lattice parameters of anatase, rutile, and pyrolusite, respectively. The unit of all the values is angstrom (Å).

Phase	Lattice parameters	
	a	*c*
Anatase (TiO_2)	3.7852	9.5139
Rutile (TiO_2)	4.5933	2.9592
Pyrolusite (MnO_2)	4.3999	2.8740

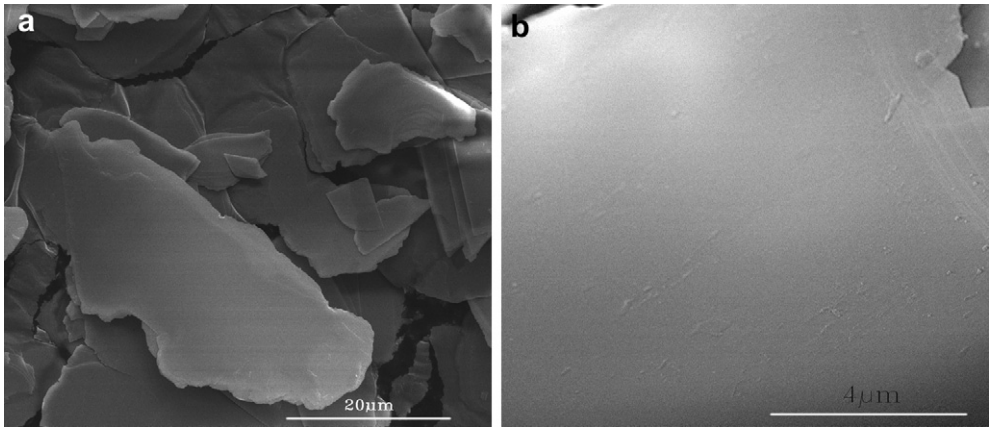

Fig. 4. (a) SEM images of mica particles, (b) higher resolution SEM image of the surface of a mica particle.

be seen from Fig. 3(b), the peaks appearing at 253, 437, and 609 cm^{-1} are typical rutile bands, and the other two weak peaks appearing at 196 and 681 cm^{-1} can be ascribed to mica. So the Raman spectra confirm that the TiO_2 coating is in the pure rutile phase when the loading of MnO_2 is increased to 2.07%, which is consistent with the XRD result.

In general, anatase–rutile transformation requires a fairly high temperature, varying from 400 to 1200 °C in a solid-state reaction [38,39]. So it is unusual to observe the transformation of anatase to rutile at the low temperature of 70 °C, for which there must be a different mechanism involved in the low temperature transformation.

In order to understand how MnO_2 affects the anatase–rutile transformation of TiO_2, crystal structures of the phases can be examined (Table 2). It can be seen that the lattice parameters of rutile and pyrolusite are strikingly close to each other along both *a* and *c* axes, while anatase has an elongated unit cell along *c*-axis and a slightly smaller unit cell along *a*-axis. Besides, rutile TiO_2 and pyrolusite both have a tetragonal structure. Therefore, MnO_2 as crystal seeds can decrease the activation energy of the reaction of formation of rutile in the liquid hydrolysis of $TiCl_4$ and promote the growth of rutile TiO_2, leading to the low temperature formation of rutile TiO_2.

3.2. Morphology of mica–titanium pigments

The SEM images of the naked mica show that the mica powder has a flaky shape with a fairly smooth surface (Fig. 4). These

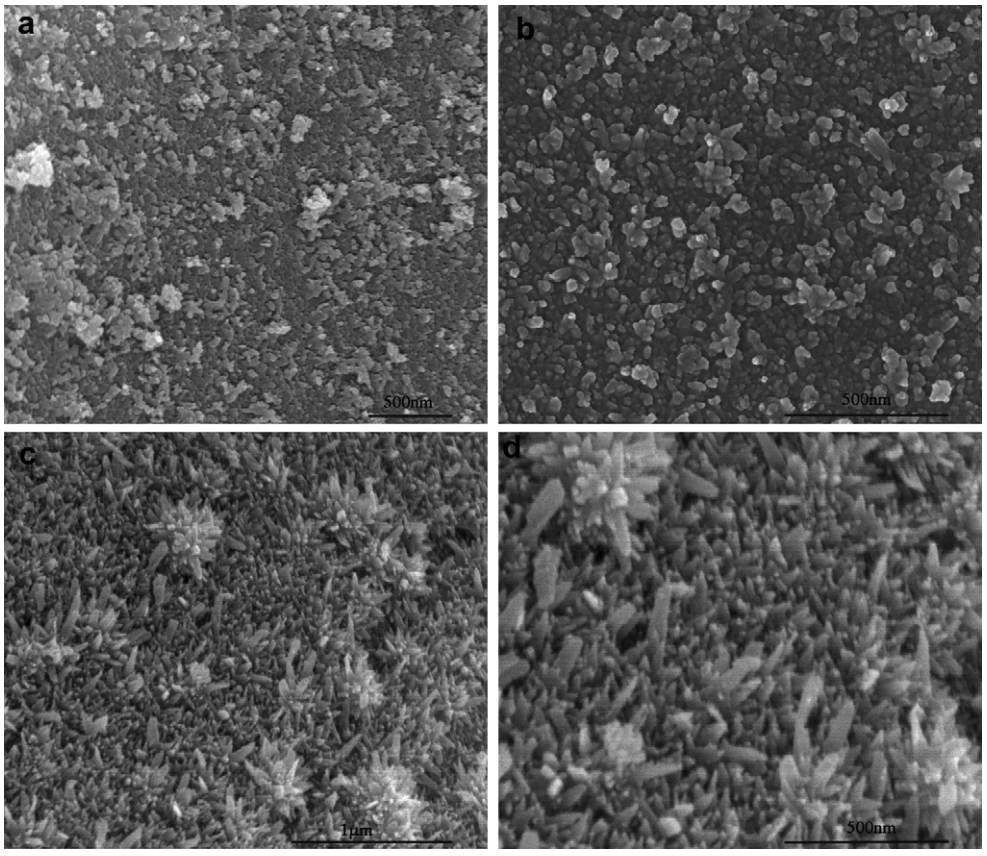

Fig. 5. SEM micrographs of mica–titanium pigments: (a,b) mica–TiO_2, (c,d) mica-2.07%MnO_2–TiO_2.

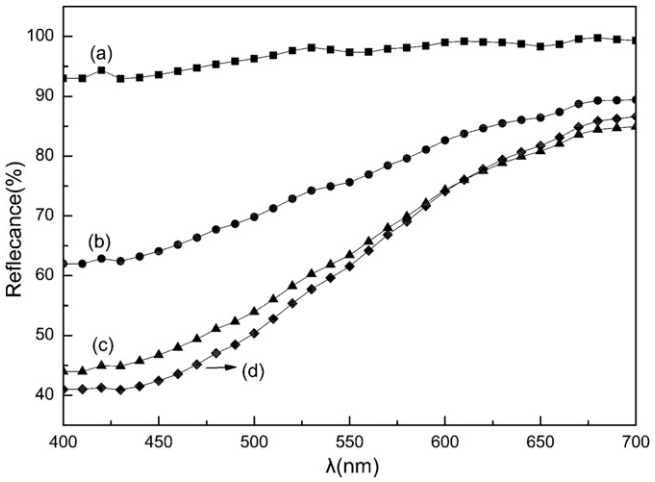

Fig. 6. The spectral reflectance curves of mica–titania pigments with different MnO_2 loadings: (a) 0, (b) 0.69%, (c) 1.38%, (d) 2.07%.

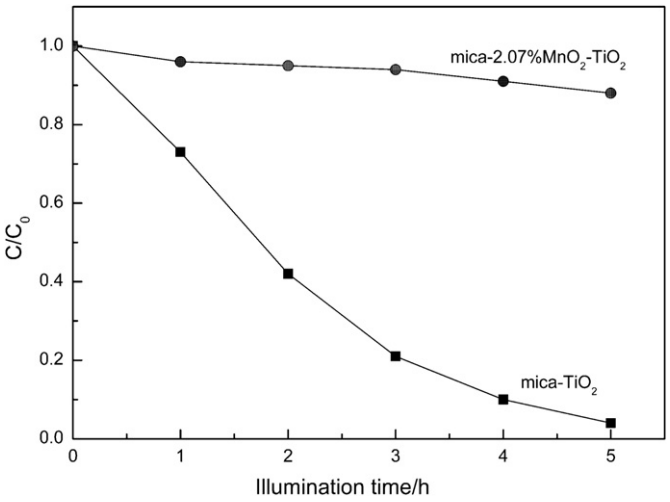

Fig. 7. The photocatalytic degradation of RhB in the presence of mica–TiO_2 and mica-2.07%MnO_2–TiO_2.

particles are of 10–70 μm in length and less than 1 μm in thickness. Fig. 5 shows SEM images of TiO_2 thin layers deposited on mica. The TiO_2 thin layers on mica for mica–TiO_2 appear to be a smooth and uniform plate. The TiO_2 coating layers are composed of anatase TiO_2 nanoparticles with an average particle size of 15 nm. However, the surface morphology changes remarkably for mica-2.07% MnO_2–TiO_2. Uniform rutile TiO_2 films are composed of highly oriented fine needles on mica surface. The diameter of the nanorods ranges from 10 to 35 nm. The film is so dense that it was difficult to evaluate the length of the nanorods. In addition nanoflower structures can be observed on the needles. These flowerlike structures are composed of many nanoplates. These nanoplates are of 23–60 nm in width and 120–240 nm in length.

3.3. Optical properties of mica–titanium pigments

Fig. 6 shows the reflectance of the mica–titanium pigments with varying MnO_2 loadings. It's clear that when the sample is not treated with any additives, the pigment shows a high reflectance in the whole visible region, so it has a white color. Then the reflectance decrease sharply in the region of 400–500 nm while remaining a high level in the region of 600–700 nm with increasing loadings of MnO_2, indicating the color becomes redder.

In order to further investigate the color characteristics of the pigments, CIE $L^*a^*b^*$ values of the pigment samples are measured. As shown in Table 3, an increase in MnO_2 loading leads to the reduction of lightness and the increase in red and saturation, which is consistent with the reflectance result.

3.4. Photocatalytic properties of mica–titanium pigments

To demonstrate the potential applicability in coatings or polymers of the as-obtained rutile TiO_2 coated mica–titanium pigments, the photocatalytic activity was investigated by examining the photocatalytic degradation of Rhodamine B (RhB). Fig. 7 shows that nearly all of the RhB was decomposed by mica–TiO_2 whilst only a small amount of RhB was degraded by mica-2.07% MnO_2–TiO_2 in 5 h. So the as-obtained rutile-TiO_2 coated mica–titanium pigments exhibit a high photostability under UV illumination, which may help to enhance the durability of organic substrates such as polymers and coatings.

Several reasons may account for the poor photocatalytic activities of rutile-TiO_2 coated mica–titanium pigments prepared in this study. First, due to rutile's slightly lower Fermi level, low capacity to absorb oxygen and lower degree of hydroxylation (i.e., number of hydroxy groups on the surface), rutile shows lower photocatalytic activity than that of anatase [40]. Moreover, Mn^{4+} may enter the crystal structure of TiO_2, which is accompanied by the formation of defects [41]. Such defects may act as the recombination center for electron–hole pair, further reducing the photocatalytic activity of rutile TiO_2.

Table 3
Color characteristics of the samples.

Sample	Color coordinates			
	L^*	a^*	b^*	C^*
Mica–TiO_2	99.07	0.15	1.99	1.99
Mica-0.69%MnO_2–TiO_2	89.97	3.20	9.30	9.84
mica-1.38%MnO_2–TiO_2	84.09	6.24	16.17	17.33
Mica-2.07%MnO_2–TiO_2	83.14	7.58	19.15	20.59

L^*, lightness; a^*, red-green index; b^*, yellow-blue index; C^*, Chroma.

4. Conclusions

Nanometer titanium dioxide (TiO_2) was deposited on mica flakes using a chemical liquid deposition method. Under normal circumstances, anatase is the crystalline phase of TiO_2 deposited, such as the mica–TiO_2 sample. Increasing amounts of MnO_2 deposited onto mica prior to TiO_2 coatings lead to an increasing mass fraction of rutile phase with respect to anatase. The use of only 2.07 wt% MnO_2 to the weight of mica was found to begin to provide a complete rutile TiO_2 coating without the need for calcination. Due to the remarkable epitaxial match between the unit cell dimensions of pyrolusite and rutile phases, MnO_2 could act as crystal seeds, favoring the low temperature formation of rutile. Moreover, MnO_2 also had a pronounced effect on the morphology of TiO_2 coatings. The prior deposition of MnO_2 onto mica lead to the formation of rutile TiO_2 films composed of highly oriented fine needles on mica surface and nanoflower structures on the needle structures. The as-obtained rutile-TiO_2 coated mica–titanium pigments are shown to exhibit a high photostability under UV illumination.

Acknowledgments

The authors thank Dr Song (Analytical and Testing Center, South China University of Technology) for kindly supporting the Raman

spectra measurement of the samples. We also thank Shaohua Wang for reflectance measurement. The work was funded by the Key Laboratory of Specially Functional Materials, South China University of Technology, Ministry of Education, China.

References

[1] Pfaff G. Special effect pigments. High performance pigments. Wiley-VCH Verlag GmbH & Co. KGaA; 2009. p. 75–104.
[2] Cho JH, Tark YD, Kim WY, Lim SH. Room-temperature synthesis and characteristics of nanocrystalline TiO_2 on mica by homogeneous precipitation. Met Mater Int 2009;15(6):1001–5.
[3] Toffidifar MR, Taheri-Nassaj E, Alizadeh P. Optimization of the synthesis of a nano-sized mica–hematite pearlescent pigment. Mater Chem Phys 2008; 109(1):137–42.
[4] Horiishi N, Kathrein H, Krieg S, Pfaff G, Pitzer U, Ronda C, et al. Specialty pigments. Industrial inorganic pigments. Wiley-VCH Verlag GmbH & Co. KGaA; 2005. p. 195–295.
[5] Pfaff G, Reynders P. Angle-dependent optical effects deriving from submicron structures of films and pigments. Chem Rev 1999;99(7):1963–82.
[6] Maile FJ, Pfaff G, Reynders P. Effect pigments – past, present and future. Prog Org Coat 2005;54(3):150–63.
[7] Kirchner E, Houweling J. Measuring flake orientation for metallic coatings. Prog Org Coat 2009;64(2–3):287–93.
[8] Tan JR, Fu XS, Hou WX, Chen XZ, Wang L. The preparation and characteristics of a multi-cover-layer type, blue mica titania, pearlescent pigment. Dyes Pigm 2003;56(2):93–8.
[9] Stengl V, Subrt J, Bakardjieva S, Kalendova A, Kalenda P. The preparation and characteristics of pigments based on mica coated with metal oxides. Dyes Pigm 2003;58(3):239–44.
[10] Cavalcante PMT, Dondi M, Guarini G, Barros FM, da Luz AB. Ceramic application of mica titania pearlescent pigments. Dyes Pigm 2007;74(1):1–8.
[11] Bayat N, Baghshahi S, Alizadeh P. Synthesis of white pearlescent pigments using the surface response method of statistical analysis. Ceram Int 2008; 34(8):2029–35.
[12] Tan JR, Shen LZ, Fu XS, Hou WX, Chen XZ. Preparation and conductive mechanism of mica titania conductive pigment. Dyes Pigm 2004;62(2):107–14.
[13] Levinson R, Berdahl P, Akbari H. Solar spectral optical properties of pigments–part II: survey of common colorants. Sol Energ Mat Sol C 2005;89(4): 351–89.
[14] Hildenbrand VD, Doyle S, Fuess H, Pfaff G, Reynders P. Crystallisation of thin anatase coatings on muscovite. Thin Solid Films 1997;304(1–2):204–11.
[15] Cho JH, Lim SH. Internal structure analysis of mica particles coated with metal oxide by transmission electron microscopy. Dyes Pigm 2006;69(3):192–5.
[16] Wang Y, Zhang L, Deng K, Chen X, Zou Z. Low temperature synthesis and photocatalytic activity of rutile TiO_2 nanorod superstructures. J Phys Chem C 2007;111(6):2709–14.
[17] Ge M, Li JW, Liu L, Zhou Z. Template-free synthesis and photocatalytic application of rutile TiO_2 hierarchical nanostructures. Ind Eng Chem Res 2011; 50(11):6681–7.
[18] Song GB, Liang JK, Liu FS, Peng TJ, Rao GH. Preparation and phase transformation of anatase–rutile crystals in metal doped TiO_2/muscovite nanocomposites. Thin Solid Films 2005;491(1–2):110–6.
[19] Zhang S, Liu C-Y, Liu Y, Zhang Z-Y, Mao L-J. Room temperature synthesis of nearly monodisperse rodlike rutile TiO_2 nanocrystals. Mater Lett 2009;63(1): 127–9.
[20] Lu A, Liu J, Zhao D, Guo Y, Li Q, Li N. Photocatalysis of V-bearing rutile on degradation of halohydrocarbons. Catal Today 2004;90(3–4):337–42.
[21] Allen NS, Edge M, Ortega A, Sandoval G, Liauw CM, Verran J, et al. Degradation and stabilisation of polymers and coatings: nano versus pigmentary titania particles. Polym Degrad Stab 2004;85(3):927–46.
[22] Allen NS, Edge M, Sandoval G, Ortega A, Liauw CM, Stratton J, et al. Interrelationship of spectroscopic properties with the thermal and photochemical behaviour of titanium dioxide pigments in metallocene polyethylene and alkyd based paint films: micron versus nanoparticles. Polym Degrad Stab 2002;76(2):305–19.
[23] Janes R, Knightley LJ, Harding CJ. Structural and spectroscopic studies of iron (III) doped titania powders prepared by sol–gel synthesis and hydrothermal processing. Dyes Pigm 2004;62(3):199–212.
[24] Wu J-M, Qi B. Low-temperature growth of rutile nanorod thin films and their photon-induced property. J Am Ceram Soc 2008;91(12):3961–70.
[25] Deluca CV, Cerce LR, Deluca C, Cerce L, Inventors. Engelhard Corporation, assignee. Rutile titanium dioxide effect pigments and production thereof. United States patent 6626989–B1, 2002 May 16.
[26] Eskelinen P, Ritala M, Leskelä M. The effect of calcination on the surface composition and structure of titanium dioxide coated mica particles. J Solid State Chem 1993;103(1):160–9.
[27] Gao Q, Wu X, Fan Y. The effect of iron ions on the anatase–rutile phase transformation of titania (TiO_2) in mica–titania pigments. Dyes Pigm 2012; 95(1):96–101.
[28] Bertaux S, Reynders P, Heintz J-M. Sintering and color properties of nanocrystalline CeO_2 films. Thin Solid Films 2005;473(1):80–8.
[29] Topuz BB, Gündüz G, Mavis B, Çolak Ü. The effect of tin dioxide (SnO_2) on the anatase–rutile phase transformation of titania (TiO_2) in mica–titania pigments and their use in paint. Dyes Pigm 2011;90(2):123–8.
[30] Zhu Y, Zhang L, Gao C, Cao L. The synthesis of nanosized TiO_2 powder using a sol–gel method with $TiCl_4$ as a precursor. J Mater Sci 2000;35(16):4049–54.
[31] Ryu YC, Kim TG, Seo GS, Park JH, Suh CS, Park SS, et al. Effect of substrate on the phase transformation of TiO in pearlescent pigment. J Ind Eng Chem 2008; 14(2):213–8.
[32] Gennari FC, Pasquevich DM. Enhancing effect of iron chlorides on the anatase–rutile transition in titanium dioxide. J Am Ceram Soc 1999;82(7):1915–21.
[33] Spurr RA, Myers H. Quantitative analysis of anatase–rutile mixtures with an X-ray diffractometer. Anal Chem 1957;29(5):760–2.
[34] Pal M, García Serrano J, Santiago P, Pal U. Size-controlled synthesis of spherical TiO_2 nanoparticles: morphology, crystallization, and phase transition. J Phys Chem C 2006;111(1):96–102.
[35] Zhang J, Li M, Feng Z, Chen J, Li C. UV Raman spectroscopic study on TiO_2. I. Phase transformation at the surface and in the bulk. J Phys Chem B 2005; 110(2):927–35.
[36] Wang C, Shao C, Liu Y, Li X. Water–dichloromethane interface controlled synthesis of hierarchical rutile TiO_2 superstructures and their photocatalytic properties. Inorg Chem 2009;48(3):1105–13.
[37] Cheng H, Ma J, Zhao Z, Qi L. Hydrothermal preparation of uniform nanosize rutile and anatase particles. Chem Mater 1995;7(4):663–71.
[38] Jung HS, Shin H, Kim J-R, Kim JY, Hong KS, Lee J-K. In situ observation of the stability of anatase nanoparticles and their transformation to rutile in an acidic solution. Langmuir 2004;20(26):11732–7.
[39] Wallot J, Reynders P, Herzing AA, Kiely CJ, Harmer MP, Rödel J. Sintering of thin film nanocrystalline titania-tin oxide composites. J Eur Ceram Soc 2008; 28(11):2225–32.
[40] Carp O, Huisman CL, Reller A. Photoinduced reactivity of titanium dioxide. Prog Solid State Chem 2004;32(1–2):33–177.
[41] Tong H, Ouyang S, Bi Y, Umezawa N, Oshikiri M, Ye J. Nano-photocatalytic materials: possibilities and challenges. Adv Mater 2012;24(2):229–51.